JACS
JOURNAL OF THE AMERICAN CHEMICAL SOCIETY

Article

pubs.acs.org/JACS

Nucleoapzymes: Hemin/G-Quadruplex DNAzyme–Aptamer Binding Site Conjugates with Superior Enzyme-like Catalytic Functions

Eyal Golub,[†] H. Bauke Albada,[†] Wei-Ching Liao, Yonatan Biniuri, and Itamar Willner*

Institute of Chemistry, The Minerva Center for Biohybrid Complex Systems, and The Center for Nanoscience and Nanotechnology, The Hebrew University of Jerusalem, Jerusalem 91904, Israel

Supporting Information

ABSTRACT: A novel concept to improve the catalytic functions of nucleic acids (DNAzymes) is introduced. The method involves the conjugation of a DNA recognition sequence (aptamer) to the catalytic DNAzyme, yielding a hybrid structure termed "nucleoapzyme". Concentrating the substrate within the "nucleoapzyme" leads to enhanced catalytic activity, displaying saturation kinetics. Different conjugation modes of the aptamer/DNAzyme units and the availability of different aptamer sequences for a substrate provide diverse means to design improved catalysts. This is exemplified with (i) The H_2O_2-mediated oxidation of dopamine to aminochrome using a series of hemin/G-quadruplex-dopamine aptamer nucleoapzymes. All nucleoapzymes reveal enhanced catalytic activities as compared to the separated DNAzyme/aptamer units, and the most active nucleoapzyme reveals a 20-fold enhanced activity. Molecular dynamics simulations provide rational assessment of the activity of the various nucleoapzymes. The hemin/G-quadruplex–aptamer nucleoapzyme also stimulates the chiroselective oxidation of L- vs D-DOPA by H_2O_2. (ii) The H_2O_2-mediated oxidation of *N*-hydroxy-L-arginine to L-citrulline by a series of hemin/G-quadruplex–arginine aptamer conjugated nucleoapzymes.

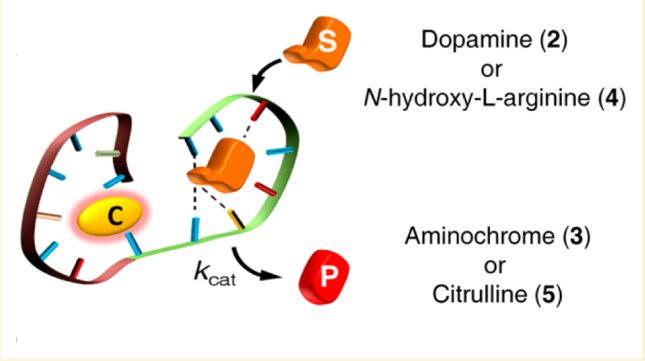

INTRODUCTION

Catalytic nucleic acids (DNAzymes) have attracted substantial research activities in recent years as a new class of bioinspired catalysts.[1,2] DNAzymes mimic the catalytic activities of enzymes and stimulate a wide variety of catalytic reactions. Besides the nicking[3] and ligating[4] of oligonucleotide substrates, they catalyze reactions such as carbon–carbon bond formation,[5] for example, Diels–Alder[6] or Michael addition[7] reactions, the phosphorylation of organic hydroxyl-groups,[8] and the oxidation of organic molecules.[9] One of the most studied DNAzymes is the hemin/G-quadruplex (hGQ) horseradish peroxidase-mimicking DNAzyme.[10] Similar to the native enzyme, the hGQ DNAzymes stimulate the H_2O_2-mediated oxidation of organic substrates to yield chromophoric[11] or fluorescent[12] products, to generate chemiluminescence in the presence of luminol,[13] or to induce the oxidation of substrates such as phenols,[14] thiols,[15] or aniline.[16] The catalytic functions of DNAzymes have been extensively implemented as amplifying labels for sensing events,[17,18] and as functional units for optoelectronic applications.[19] In spite of tremendous research efforts, artificial DNAzyme catalysts that operate on non-nucleotide substrates usually exhibit inferior catalytic activities as compared to native enzymes. This might originate from the fact that such DNAzymes typically lack binding affinities for those substrates. A possible approach to improve the catalytic function of such DNAzymes rests on the tremendous progress achieved in the study of ligand-binding DNA sequences (i.e., aptamers).[20,21] The aptamers, selected via the SELEX process, display ligand-specific affinity properties toward various substrates, including low-molecular-weight molecules, macromolecules, and even cells. Accordingly, aptamers have been widely applied for selective sensing and for biomedical and nanotechnological applications.[22,23] Thus, we postulated that the conjugation of a DNAzyme sequence as an active site, and an aptamer as a binding site could form a functional hybrid conjugate that mimics enzymes by concentrating the substrate in close proximity to the active site, Figure 1A. Although a few examples demonstrated the cooperative binding and catalytic activity within nucleic acid sequences,[24,25] our approach seems to be more general due to the modular conjugation of an aptamer and a DNAzyme. In the present approach, the DNAzyme–aptamer hybrid structures, which we term "nucleoapzymes", encompass several innovative features: (i) The aptamer unit can be linked to the DNAzyme unit at different positions, thus providing a means to generate different biocatalytic structures with tailored activities. (ii) The linker that connects the aptamer unit with the DNAzyme unit can be varied, thus allowing modulation of the structural features of the resulting aptamer-DNAzyme conjugate, thereby controlling

Received: September 15, 2015
Published: December 13, 2015

DOI: 10.1021/jacs.5b09457
J. Am. Chem. Soc. 2016, 138, 164–172

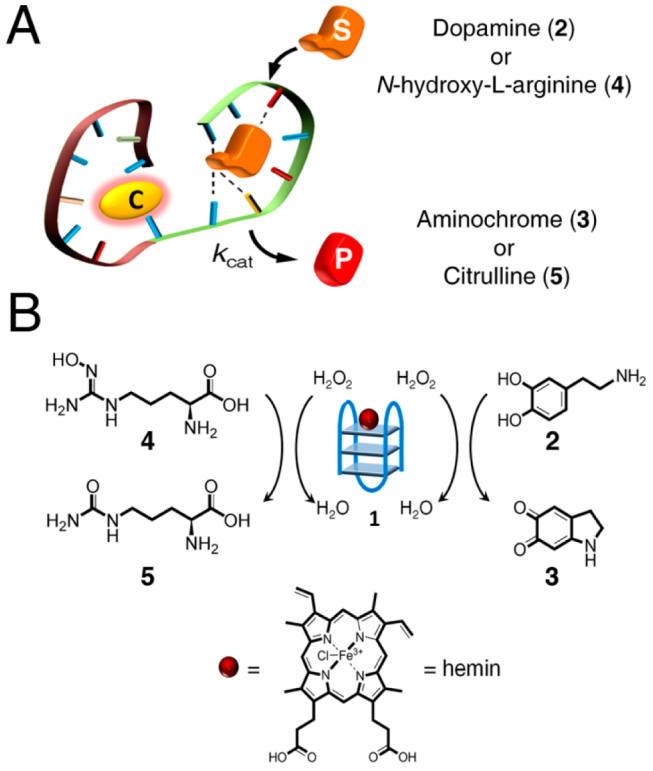

Figure 1. (A) Schematic general model of a catalytic "nucleoapzyme" hybrid structure. The system consists of a binding site formed by the aptamer unit (green) and a catalytic DNAzyme unit (red) containing a catalytic site (C). Binding of the substrate (S) to the aptamer exposes the substrate to the catalytic site, and the generated product (P) reveals low affinity toward the aptamer, resulting in its release from the "nucleoapzyme". (B) The hGQ-catalyzed H_2O_2-stimulated oxidation of dopamine (**2**) to aminochrome (**3**) and the hGQ-catalyzed oxidation of *N*-hydroxy-L-arginine (**4**) to L-citrulline (**5**).

its activity. (iii) The binding site of the aptamer provides a chiral environment, which allows chiroselective binding and catalysis. We note that this novel concept of "nucleoapzymes" should not be confused with the already described "aptazymes".[26] Whereas in aptazymes the recognition of a ligand by the aptamer unit allosterically regulates the catalytic functions of the DNAzyme (operating on a nonligand substrate), in nucleoapzymes the non-nucleotide ligand that binds to the aptamer-part of the oligonucleotide acts as the substrate for the DNAzyme. It should be noted that the tailored proximity between the DNAzyme and aptamer units might be designed by other means, such as duplex or triplex alignment of the DNAzyme/aptamer units or supramolecular interaction between the units, for example, micellar structures of lipido-DNAzyme/lipido-aptamer units. Furthermore, the DNAzyme catalytic site within the nucleoapzymes may be substituted by synthetic catalysts, thus allowing the stimulation of many different reactions. That is, the structural diversity of nucleoapzymes might provide a rich platform for enzyme-mimicking catalysts.

Here we wish to report on an innovative approach to enhance the catalytic performance of DNAzymes that operate on non-nucleotide substrates. We first report on two new hGQ (**1**)-catalyzed reactions, Figure 1B, namely, the H_2O_2-assisted oxidation of dopamine (**2**) to aminochrome (**3**) and the oxidation of *N*-hydroxy-L-arginine (**4**) to L-citrulline (**5**). Then, we implement the concept of nucleoapzyme by designing appropriate hGQ–aptamer conjugates for these reactions as functional hybrids for the enhanced oxidation of the respective substrates. This study highlights the following general accomplishments: (i) The conjugation of the dopamine-binding aptamer, DBA (**6**), or of the arginine aptamer (exhibiting binding affinity toward *N*-hydroxy-L-arginine, *vide infra*) as a binding site to the hGQ catalytic site yields nucleoapzymes exhibiting enhanced catalytic activities as compared to the separated hGQ and aptamer units and display enzyme-like saturation kinetics with multiple turnovers. (ii) The different configurations of the nucleoapzymes yield structure-dependent catalytic activities. We rationalize the relative activities of the nucleoapzymes by molecular dynamics simulations that provide insight into the structure–function relationships in the hybrid nucleoapzymes. In our discussion, we address separately the two different nucleoapzyme-catalyzed reactions. It should be noted that a recently reported related study has implemented a phosphorylation DNAzyme conjugated to an ATP aptamer as a scaffold for the catalytic phosphorylation of a tyrosine-containing peptide within a supramolecular oligonucleotide structure.[27] This system showed, however, a single turnover since the product was not separable from the catalytic conjugate.

RESULTS AND DISCUSSION

For the first system, the oxidation of dopamine to aminochrome, the DBA (**6**)[28,29] and the hGQ provided the binding and catalytic units, respectively, for the construction of the dopamine-oxidizing nucleoapzymes. The fact that dopamine is oxidized by horseradish peroxidase in the presence of H_2O_2[30] suggested that the hGQ could, similarly, act as catalyst for this oxidation reaction, Figure 1B. Indeed, we find that hGQ catalyzes the oxidation of dopamine (**2**) to (**3**) by H_2O_2 (*vide infra*). Accordingly, we designed a series of hGQ/DBA conjugates as nucleoapzymes for the enhanced oxidation of dopamine (**2**), Figure 2A. Within this series of nucleoapzymes, we highlight the following features: (i) All nucleoapzymes reveal enhanced activities as compared to the separated hGQ and DBA units. (ii) The relative activities of the nucleoapzymes depend on the structures of hGQ/DBA conjugates; the activities are rationalized by molecular dynamics simulations. (iii) The oxidation of L- or D-DOPA, exhibiting binding affinities toward the DBA, reveals chiroselective oxidation in the presence of the hGQ/DBA nucleoapzyme.

The H_2O_2-mediated hGQ-catalyzed oxidation of dopamine (**2**) to aminochrome (**3**), Figure 1B, was studied by monitoring the time-dependent absorbance changes of the reaction product, Figures S1 and S2, Supporting Information. We found that the hGQ catalyzes the oxidation of dopamine (**2**) to aminochrome (**3**) with a comparable rate to a similar system that contained both hGQ and DBA, Figure S2, curves (a) and (b), respectively. Furthermore, the oxidation of dopamine by hemin only, either in the presence or absence of the DBA strand, resulted in a very low background signal. These control experiments give important insights into the system: (i) The hGQ structure catalyzes the oxidation of dopamine (**2**) to (**3**) by H_2O_2. (ii) The added aptamer does not affect the rate of oxidation of dopamine (**2**) to (**3**) by hGQ in the presence of H_2O_2. (iii) Hemin itself was not an efficient catalyst for this reaction. Using the highly programmable nature of DNA, different nucleoapzyme configurations were designed, Figure 2A. These included nucleoapzymes, where the hGQ DNAzyme was linked either to the 5′- or 3′-end of the DBA,

DOI: 10.1021/jacs.5b09457
J. Am. Chem. Soc. 2016, 138, 164–172

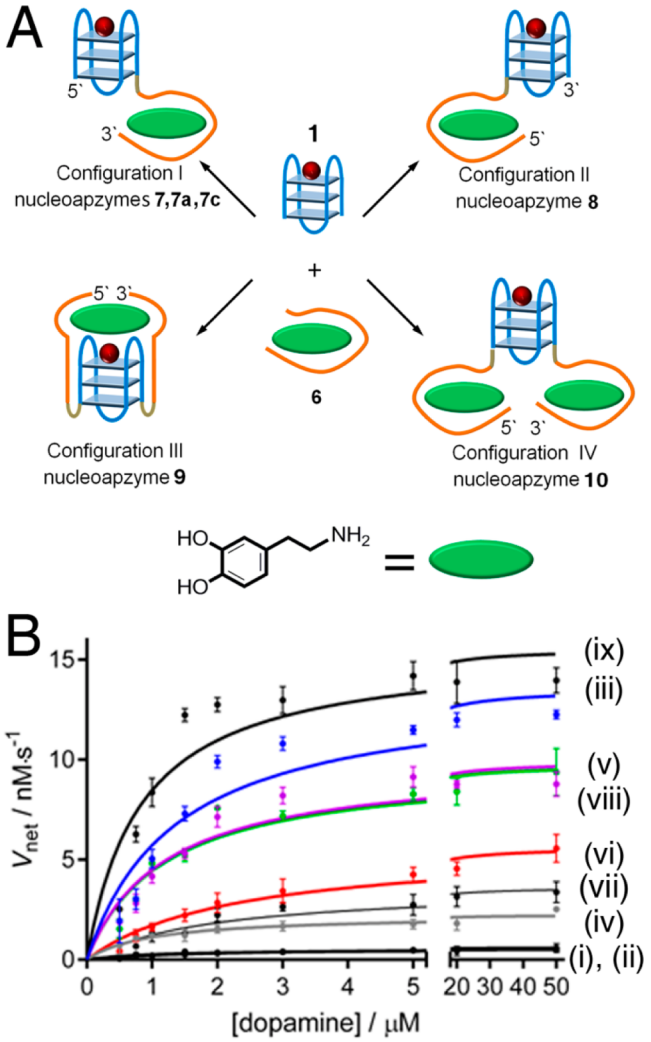

Figure 2. (A) Schematic presentation of the four different nucleoapzyme configurations implemented in this study. (B) Saturation curves corresponding to the oxidation rate of dopamine to aminochrome at variable concentrations of dopamine, in the presence of (i) separated hGQ (**1**) and DBA (**6**) components, (ii) hGQ alone, (iii) nucleoapzyme **7**, (iv) nucleoapzyme **8**, (v) nucleoapzyme **9**, (vi) mutated nucleoapzyme **7a**, (vii) scrambled sequence **7b**, (viii) nucleoapzyme **7c**, and (ix) nucleoapzyme **10**. V_{net} corresponds to $V_{obs} - V_{hemin}$.

configurations I (**7**) and II (**8**), respectively, and a nucleoapzyme, where the DBA was split into two subunits that were linked to both sides of the G-quadruplex sequence, resulting in a "middle"-positioned DNAzyme, configuration III (**9**). The catalytic oxidation of dopamine (**2**) to aminochrome (**3**) by each of the nucleoapzyme configurations was examined and compared to the catalytic oxidation of dopamine by the separated DNAzyme/DBA units, Figure 2B. We observed that all nucleoapzyme conjugates revealed enhanced oxidation rates for the oxidation of (**2**) to (**3**) by H_2O_2, as compared either to the separated hGQ/DBA or to the hGQ systems, curves (i) and (ii), respectively. Whereas the oxidation rate of dopamine by the separated DBA and DNAzyme units increases linearly with the concentration of the substrate, following second order rate kinetics with $k_2 = (0.9 \pm 0.1) \times 10^{-3}$ s^{-1}, Figure 2B, curve (i), the different nucleoapzymes not only exhibited enhanced oxidation rates, but also show typical saturation kinetics, Figure 2B. Accordingly, the oxidation rates of dopamine (**2**) to aminochrome (**3**) by H_2O_2 in the presence of the different nucleoapzymes were analyzed in terms of the Michaelis–Menten model,[31] eq 1:

$$v = \frac{V_{max}[S]}{K_M + [S]} \quad (1)$$

where v is the rate of oxidation, [S] is the substrate concentration, and K_M is the Michaelis constant, which corresponds to the substrate concentration at which $v = 0.5V_{max}$ (Table 1).

Interestingly, the different nucleoapzyme configurations differ in their catalytic performance. Nucleoapzyme **7** reveals the highest rate of oxidation, curve (iii), whereas nucleoapzyme **8** shows the lowest catalytic performance, curve (iv), and nucleoapzyme **9** shows an intermediate activity, curve (v). Table 1 summarizes the kinetic parameters characterizing the different nucleoapzyme structures. The nucleoapzymes **7** and **8** exhibit k_{cat} and K_M values corresponding to $(18.3 \pm 0.9) \times 10^{-3}$ s^{-1}, (1.3 ± 0.1) μM, and $(3.1 \pm 0.1) \times 10^{-3}$ s^{-1}, (0.9 ± 0.1) μM, respectively, revealing 20-fold and 3-fold enhancement, respectively, as compared to the system composed of the separated components. Nucleoapzyme **9** exhibits k_{cat} and K_M values of $(13.2 \pm 0.6) \times 10^{-3}$ s^{-1} and (1.2 ± 0.2) μM, respectively, which corresponds to a 15-fold enhancement factor.

These results imply that the DBA unit of the nucleoapzyme is indeed involved in the oxidation reaction by concentrating the dopamine substrate in close proximity to the DNAzyme active site, most likely via a random sequential mechanism that leads to the catalytically active ternary complex, Figure S3.[32] Thus, at higher concentrations of dopamine the DBA becomes saturated, and the oxidation rate is limited by the turnover frequency of the DNAzyme. It should be noted that the

Table 1. Kinetic Parameters of the Various DBA-hGQ Nucleoapzymes with Respect to the Oxidation of Dopamine to Aminochrome[a]

entry	nucleoapzyme	k_{cat} (10^{-3} s^{-1})	K_M (μM)	k_{cat}/K_M (10^{-3} $s^{-1}\cdot\mu M^{-1}$)	V_{max} (nM·s^{-1})	k_{cat}/k_2
1	5′-TATA (**7**)	18.3 ± 0.9	1.3 ± 0.1	14.1	13.5 ± 0.5	20
2	3′-TATA (**8**)	3.1 ± 0.1	0.9 ± 0.1	3.4	2.3 ± 0.2	3
3	middle (**9**)	13.2 ± 0.6	1.2 ± 0.2	11.0	9.8 ± 0.5	15
4	mutant (**7a**)	7.7 ± 0.4	2.0 ± 0.3	3.8	5.7 ± 0.6	8
5	scrambled (**7b**)	4.4 ± 0.4	2.0 ± 0.4	2.4	3.4 ± 0.6	5
6	5′-A (**7c**)	13.0 ± 0.7	1.2 ± 0.2	10.8	9.6 ± 0.5	14
7	DBA-GQ-DBA (**10**)	20.7 ± 1.2	0.8 ± 0.2	25.9	15.3 ± 0.5	23

[a]Conditions: 0.5–50 μM dopamine, 100 μM H_2O_2, 0.74 μM nucleoapzyme, buffer: 5 mM MES, pH = 5.5, 200 mM $NaNO_3$, 20 mM KNO_3, and $Mg(NO_3)_2$, 5 mM. Notes: the rate constant for the hGQ DNAzyme (**1**) is $k_2 = (0.9 \pm 0.1) \times 10^{-3}$ s^{-1}. $k_{cat} = V_{max}/0.74$.

DOI: 10.1021/jacs.5b09457
J. Am. Chem. Soc. 2016, 138, 164–172

characteristic absorption band of the hGQ unit in all nucleoapzyme configurations is similar and remains unchanged during the entire course of the reactions (see Figure S4). This reveals that the formation of the catalytically active hGQ DNAzyme is not perturbed in the different nucleoapzymes and that it remains stable during the reaction. We also note that the activities of the hGQ units in the different nucleapzymes, toward the oxidation of an aptamer independent substrate, for example, the oxidation of 2,2′-azino-bis(3-ethylbenzothiazoline-6-sulfonic acid), $ABTS^{2-}$, by H_2O_2 are identical. Therefore, the aptamer unit does not affect the hGQ activity.

To assess the significance of the dopamine binding site for the enhanced activity of the different nucleoapzymes, we performed a series of complementary experiments: (i) Fluorescence anisotropy measurements revealed similar binding affinity of dopamine (**2**) to nucleoapzymes **7** and **8** as compared to DBA alone, whereas nucleoapzyme **9** revealed a ca. 15% lower affinity; see Table S1 and accompanying disscusion, Supporting Information. Thus, the enhanced catalytic activity of the nucleoapzymes does not originate from an increase in the affinity of dopamine (**2**) to the nucleoapzyme structures. (ii) Previous studies have identified several nucleotide residues in the DBA domain that are likely to participate in the binding to dopamine[28,29] and have also demonstrated that mutating them reduces the affinity of dopamine toward the aptamer.[33] Accordingly, we mutated the DBA binding residues of nucleoapzyme **7** to thymine units that yields the mutated nucleoapzyme (**7a**) that exhibited a lower affinity to dopamine, as was confirmed by fluorescence anisotropy analysis. Evidently, the mutated nucleoapzyme (**7a**) reveals a 2.5-fold decrease in activity as compared to **7**, Figure 2B curves (vi) and (iii), respectively (for the kinetic parameters characterizing the nucleoapzyme (**7a**), see Table 1). (iii) We attached to the hGQ unit a scrambled oligonucleotide chain that includes the same base content and length as the DBA, structure **7b**. Indeed, the catalytic activity exhibited by this structure, Figure 2B curve (vii) and Table 1 entry 5, is substantially lower than the rate of oxidation of dopamine (**2**) in the presence of **7**. These results demonstrate the significance of the DBA sequence both for the binding of the dopamine substrate and concentrating it within the nucleoapzyme structures adjacent to the hGQ catalytic site, thus leading to an enhanced catalytic activity. It should be noted that the catalytic activity of **7b**, that was anticipated to reveal catalytic activities similar to the separated hGQ/aptamer system, shows a slightly higher activity than expected. Although this is not yet fully understood, this might be attributed to a side effect of the nucleic acid tether on the activity of the hGQ catalyst[34] (a similar effect was observed in the cross reactivity studies, *vide infra*) and in fact a recent study highlighted the effects of aptamer tethers on the activity of hGQ.[35] However, we find only a minute influence of the DNA tether on the activity of the hGQ that cannot account for the enhanced catalysis observed in our systems.

To account for the different catalytic activities of nucleoapzymes in configurations I, II, and III, we have implemented molecular dynamics simulations using the YASARA Structure software package.[36,37] Previous studies have successfully applied this software for the computational analysis of aptamer-ligand complexes.[38] Accordingly, we have applied the method to generate a plausible structural model for the aptamer-dopamine complex (for details, see Experimental Section and Supporting Information). The computational simulations suggest the formation of an asymmetrical barrel-shaped binding pocket where the wider rim of the barrel faces the 5′-end of the aptamer, while the narrow rim faces the 3′-end of the aptamer (Figure S5). According to these simulations dopamine can bind to the barrel-shaped binding site via the wide rim while its binding via the narrow rim is prohibited. In the next step, we conjugated the hGQ to the aptamer structure to yield configurations I, II, and III. The computed structures of nucleoapzymes **7**, **8**, and **9** are displayed in Figure 3. We find that molecular dynamics simulations of configuration I yield a stable structure where the hGQ faces the wide opening of the binding sites, whereas in configuration II the hGQ faces the hindered side of the binding pocket. In configuration III, the hGQ also faces the open region of the binding pocket, yet it occupies a more distal position as compared to configuration I. The approximate distances separating the hGQ site and the DBA site are indicated in Figure 3. Based on the above observations, we further attempted to improve the functions of the nucleoapzyme **7** by conjugating the hGQ to the 5′-end of the DBA by a shorter linker. As the tether between the DBA and the DNAzyme is very flexible, we argued that a shorter linkage would increase the activity of the nucleoapzyme by reducing the distance between binding site and catalytic site. Therefore, we constructed nucleoapzyme **7c**, in which a single adenosine nucleotide links the two units. This intuitive process did not lead, however, to the expected results. The rate of dopamine oxidation is only 14-fold higher as compared to the separated DBA and DNAzyme units, Figure 2B, curve (viii) and Table 1, entry 6. This is lower than the 20-fold enhanced activity that was determined for nucleoapzyme **7**, Figure 2B, curve (ii) and Table 1, entry 1. The molecular dynamics simulations revealed, however, that although the entire hGQ unit is in closer proximity to the dopamine-binding site, the short tether limits the conformational flexibility of the DNAzyme and forces the unit to rotate and accommodate a perturbed position with respect to the binding site (Figure S6). In effect, the shorter spacer forces the catalytic site of the DNAzyme to occupy a position in the nucleoapzyme structure that is less favorable for the oxidation reaction. For larger figures of the models, see Figures S6−S9, Supporting Information.

We have further examined the catalytic performance of a hGQ DNAzyme conjugated at both its 3′- and 5′-end to a DBA, Figure 2A, configuration IV, nucleoapzyme **10**. The tethering of two aptamer units to the hGQ yields an additive enhancement in the biocatalytic process, Figure 2B, curve (ix), with the calculated $k_{cat} = (20.7 \pm 1.2) \times 10^{-3}\ s^{-1}$ corresponding to a 23-fold enhancement. Indeed, the activity of nucleoapzyme **10** is as high as that of nucleoapzymes **7** and **8** combined. This result suggests that by implementing scaffolds for the organization of dendritic hGQ/DBA conjugates the dopamine oxidation reaction could be further enhanced.

The DBA is known to reveal binding affinities (albeit lower) to other catechol derivatives such as 3,4-dihydroxyphenylalanine, DOPA.[28] Thus, we argued that the diastereoisomeric interactions between L-DOPA and D-DOPA with the DBA could lead to the chiroselective oxidation of the DOPA enantiomers by H_2O_2. Accordingly, nucleoapzyme **7** was implemented in the H_2O_2-mediated nucleoapzyme-catalyzed oxidation of L- or D-DOPA (**11a** or **11b**, respectively) to L- and D-dopachrome (**12a** or **12b**, respectively), respectively, Figure 4A. Figure 4B, curves (i) and (ii), depicts the rate of oxidation of variable concentrations of L- and D-DOPA, respectively, by

DOI: 10.1021/jacs.5b09457
J. Am. Chem. Soc. 2016, 138, 164−172

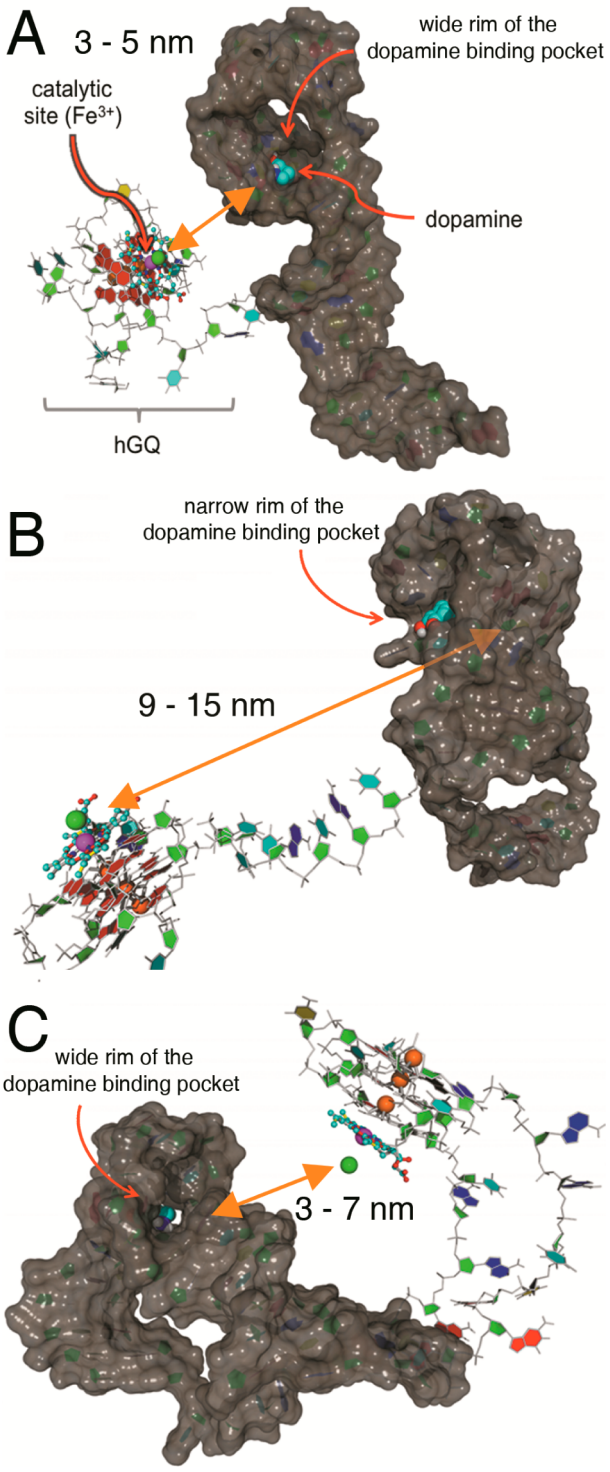

Figure 3. Computer-generated models of nucleoapzymes: (A) **7**, (B) **8**, and (C) **9**. The catalytic site and dopamine-binding site are indicated, as well as a docked dopamine substrate. The catalytically active Fe^{III}-ion of the hemin groups is shown as a purple sphere (the porphyrin is shown in the ball-and-stick representation), with its chloride counterion (green sphere); also shown are the K^+-ions that stabilize the G-quadruplex structure (orange spheres, the entire G-quadruplex is shown in the stick representation). For clarity, furanose-rings are green, and the rings of the bases are colored with A (blue), T (teal), C (yellow), and G (red). The range corresponding to the distance between the hGQ and DBA units is indicated for each of the configurations. Larger versions of these models are found in the Supporting Information.

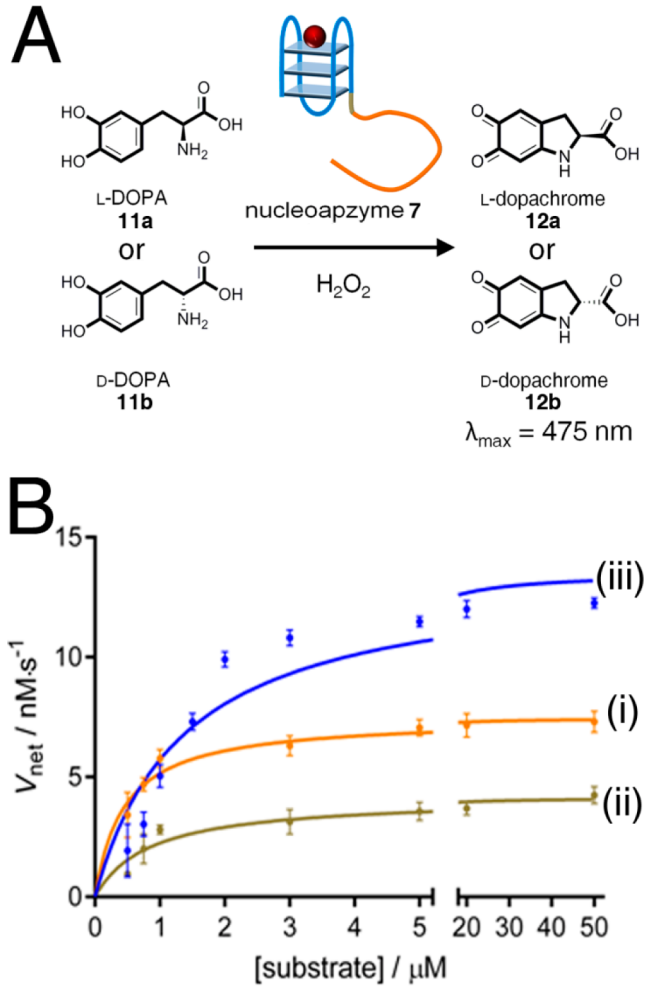

Figure 4. (A) Nucleoapzyme **7**-catalyzed H_2O_2-mediated oxidation of L-DOPA (**11a**) or D-DOPA (**11b**) to L-dopachrome (**12a**) or D-dopachrome (**12b**), respectively. (B) Kinetic curves of the **7**-catalyzed H_2O_2-mediated oxidation rate of: (i) L-DOPA (**11a**), (ii) D-DOPA (**11b**), and (iii) dopamine (**2**).

H_2O_2, in the presence of nucleoapzyme **7**. For comparison, the results for the oxidation of dopamine (**2**) are also depicted, Figure 4B, curve (iii). Indeed, the calculated catalytic rate constants for L- and D-DOPA, k_{cat} = (10.1 ± 0.4) × 10^{-3} s^{-1} and (5.2 ± 0.4) × 10^{-3} s^{-1}, respectively, indicate that the oxidation of L-DOPA (**11a**) by nucleoapzyme **7** is faster than the oxidation of its D-enantiomer (**11b**) (Table 2). This difference in catalytic activity is reasoned by the lower K_M values for L-DOPA, implying a stronger affinity of L-DOPA for the aptamer-unit as compared to D-DOPA. Based on the specificity constants, a 2.5-fold higher specificity toward L-DOPA can be calculated. It should be noted, however, that the resulting V_{max} for both substrates is still lower than that for dopamine, showing that nucleoapzyme **7** is better-suited to oxidize dopamine rather than L- and D-DOPA. This is most likely due to the higher affinity of dopamine for the aptamer. Also, the oxidation of L- and D-DOPA, in the presence of H_2O_2 and the separated hGQ-aptamer units, or by the hGQ alone, or by the hGQ in the presence of a foreign nucleic acid, did not show any chiroselectivity, implying that the diastereomeric interactions of L- and D-DOPA with the nucleoapzyme lead to the observed chiroselectivity.

DOI: 10.1021/jacs.5b09457
J. Am. Chem. Soc. 2016, 138, 164−172

Table 2. Kinetic Parameters for the Oxidation of L- and D-DOPA by Nucleoapzyme 7[a]

substrate	k_{cat} (10^{-3} s^{-1})	K_M (μM)	k_{cat}/K_M (10^{-3} $s^{-1}\cdot\mu M^{-1}$)	V_{max} (nM·s^{-1})
L-DOPA (**11a**)	10.1 ± 0.4	0.42 ± 0.1	24.0	7.4 ± 0.2
D-DOPA (**11b**)	5.2 ± 0.4	0.73 ± 0.2	7.1	3.9 ± 0.2

[a]Conditions: 0.5−50 μM substrate, 100 μM H_2O_2, 0.74 μM nucleoapzyme 7, buffer: 5 mM MES, pH = 5.5, 200 mM $NaNO_3$, 20 mM KNO_3. Note: $k_{cat} = V_{max}/0.74$.

For the second system we studied the hGQ-catalyzed oxidation of *N*-hydroxy-L-arginine by H_2O_2 to form L-citrulline using different nucleoapzyme structures, Figure 5A. Three different arginine binding aptamers (RBA) are known: 1DB6 (**13**),[39] 1OLD, (**14**),[40] and 2ARG (**15**).[41] We found that *N*-hydroxy-L-arginine exhibits binding affinities to the three arginine aptamers in the order of 1DB6 (**13**) > 2ARG (**15**) > 1OLD (**14**), with the following approximate values: $K_a = 2 \times 10^4$ M^{-1}; $K_a = 1.6 \times 10^3$ M^{-1}; $K_a = 4 \times 10^2$ M^{-1}, respectively.

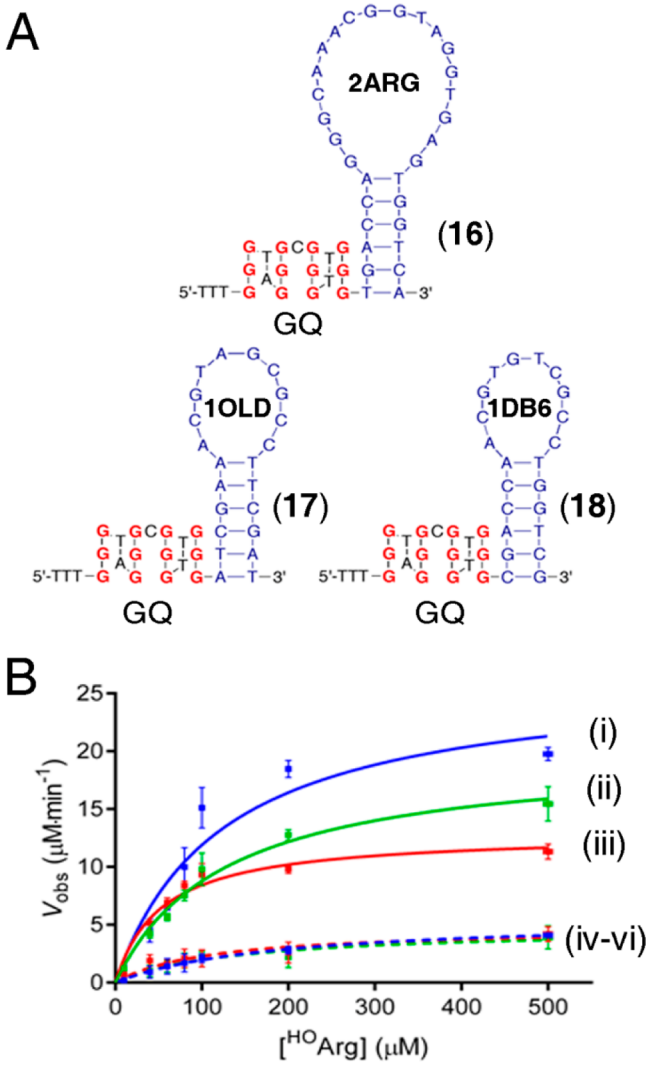

Figure 5. (A) Three nucleoapzyme structures implemented for the oxidation of *N*-hydroxy-L-arginine to L-citrulline; the aptamer unit is depicted in blue, and the hGQ DNAzyme unit in red. (B) Saturation kinetic curves of the oxidation of *N*-hydroxy-L-arginine to L-citrulline by means of three different nucleoapzymes: (i) hGQ-2ARG (**16**), (ii) hGQ-1OLD (**17**), and (iii) hGQ-1DB6 (**18**), or in the presence of the separated hGQ/aptamer components: (iv) 2ARG/hGQ, (v) 1OLD/hGQ, and (vi) 1DBG/hGQ.

Based on the nucleoapzyme approach this aptamer diversity gave us the opportunity to design different hGQ−aptamer conjugates for a single reaction and to test the general applicability of the approach. Accordingly, we designed three nucleoapzymes structures, depicted in Figure 5A, consisting of the different aptamers linked through their 5′-end to the 3′-end of the hemin/G-quadruplex. Note that in these systems we conjugated only the 5′-end of the aptamers, due to the hairpin structure of the aptamer. Figure 5B shows the rates of L-citrulline formation by the hGQ-2ARG nucleoapzyme (**16**) curve (i), hGQ-1OLD nucleoapzyme (**17**) curve (ii), and hGQ-1DB6 nucleoapzyme (**18**) curve (iii). We compared the activities of the different nucleoapzymes to the activities of the separated hGQ/2ARG, hGQ/1OLD and hGQ/1DB6 units, Figure 5B curves (iv), (v), and (vi), respectively. While all separated hGQ/aptamer systems show a linear increase with the concentration of *N*-hydroxy-L-arginine, all nucleoapzyme-catalyzed processes reveal saturation-type kinetics that is consistent with saturation of the binding site of the nucleoapzyme structure by the substrate. The most active nucleoapzyme, hGQ-2ARG (**16**), showed a 6.4-fold increase in the oxidation rate of *N*-hydroxy-L-arginine in comparison to the oxidation of the substrate by the separated hGQ and 2ARG aptamer units: $k_{cat} = (598 \pm 96) \times 10^{-3}$ s^{-1} vs $k_{cat} = (93 \pm 7) \times 10^{-3}$ s^{-1}, respectively, Table 3, entry 1. A 4- and 3.1-fold enhanced catalytic performance was observed for the nucleoapzymes (**17**) and (**18**), with $k_{cat} = (449 \pm 30) \times 10^{-3}$ s^{-1} and $k_{cat} = (291 \pm 22) \times 10^{-3}$ s^{-1}, respectively, when compared to the separate units, Table 3, entries 2 and 3. Structures of the different hGQ-aptamer nucleoapzymes, obtained by molecular dynamics simulations, are depicted in Figure S10, Supporting Information. All structures indicate the proximity of the binding site with respect to the catalytic hGQ site. It should be noted that the catalytic activities of the hGQ-RBA do not follow the same trend as that of the binding affinities toward *N*-hydroxy-L-arginine, (**4**). This reinforces our conclusion that the activities of the nucleoapzymes are controlled not only by the affinity interactions between the substrate and the aptamer binding sites, but also by other parameters such as the proximity between the catalytic site and the binding site, the alignment of the catalytic site in respect to the binding site, and the rigidity of the nucleoapzyme structure. Nonetheless, future mutations of the RBAs and complementary activity studies could shed light on the activity differences.

In this study, we have developed nucleoapzymes for two different reactions. Importantly, these structures contain an identical active site but differ in their binding sites. To demonstrate the importance of conjugated aptamer unit for the specificity of the resulting nucleoapzymes, we examined the cross-reactivity features of the hGQ-DBA (**7**) and the hGQ-RBA, (**16**), (**17**), and (**18**) nucleoapzymes, Table S2. Indeed, the oxidation rate of *N*-hydroxy-L-arginine (**4**) by the hGQ-DBA nucleoapzyme (**7**) in the presence of H_2O_2 was only slightly higher than that observed for the hGQ alone. Additionally, the activities of nucleoapzymes (**16**), (**17**), or

DOI: 10.1021/jacs.5b09457
J. Am. Chem. Soc. 2016, 138, 164−172

Table 3. Kinetic Parameters of RBA-hGQ Nucleoapzymes (16)−(18) with Respect to the Oxidation of *N*-Hydroxy-L-arginine to L-Citrulline[a]

entry	nucleoapzyme	k_{cat} (10^{-3} s^{-1})	K_M (μM)	k_{cat}/K_M (10^{-3} $s^{-1}\cdot\mu M^{-1}$)	V_{max} (μM·min^{-1})	k_{cat}/k_2
1	5′-hGQ-2ARG (**16**)	598 ± 96	123.3 ± 46	4.9 ± 0.2	26.6 ± 4.3	6.4
2	5′-hGQ-1OLD (**17**)	449 ± 30	127.3 ± 20	3.5 ± 0.2	19.9 ± 1.3	4.8
3	5′-hGQ-1DB6 (**18**)	291 ± 22	53.0 ± 12	5.4 ± 0.1	12.9 ± 10	3.1

[a]Conditions: 10−500 μM *N*-hydroxy-L-arginine, 1 mM H_2O_2, 0.74 μM nucleoapzyme, buffer: 100 mM HEPES, 200 mM KCl, 2 mM $MgCl_2$, pH 8.4. Notes: The rate constant for the hGQ DNAzyme (**1**) is $k_2 = (93 \pm 7) \times 10^{-3}$ s^{-1}. $k_{cat} = V_{max}/0.74$.

(**18**) for the oxidation of dopamine to aminochrome were comparable to that of the hGQ. These results highlight the selectivity of activities of the different nucleoapzyme structures for their respective substrates and the unique catalytic properties that emerge from the programmed organization of the hGQ−aptamer hybrid conjugates.

CONCLUSIONS

In conclusion, the present study introduces an innovative approach to improve the catalytic activities of DNAzymes via the conjugation of the DNAzyme catalytic unit to the aptamer binding sites. This is exemplified by the catalytic oxidation of dopamine and *N*-hydroxy-L-arginine to aminochrome and L-citrulline, respectively. Importantly, the study shows that the catalytic performance of the nucleoapzymes is controlled by their configuration, and by introducing mutations into the conjugates. Furthermore, molecular dynamics simulations of the DBA-DNAzyme configurations corroborated our experimental results. This provides exciting new opportunities to implement computational means to predict and tailor the catalytic functions of nucleoapzyme structures. We emphasize, however, that the concept is, at present, exemplified for hGQ−aptamer hybrids linked via covalent conjugation between the units. The possibility to extend this concept to other DNAzyme−aptamer structures, for example, duplex/triplex DNAzyme−aptamer assemblies, micellar or dendritic aptamer−DNAzyme structures, or even substitution of the DNAzyme moiety by molecular catalysts[42] might provide exciting opportunities for developing catalytic nucleic acid structures. Furthermore, such nucleoapzyme structures may be applied as effective catalysts for sensing applications.

EXPERIMENTAL SECTION

Materials. The hemin was purchased from Frontier Scientific and was dissolved in DMSO to generate a freshly prepared stock solution of 1 mM. All other materials used in this study were purchased from Sigma and were used without any additional purification. All nucleic acids were purchased from Integrated DNA Technologies (IDT). In the primary sequences listed below, the G-quadruplex sequence is *italic*, the DBA is **bold**, the arginine aptamer is ***bold-italic***, and the linker is normal text. Nucleotides participating in the dopamine binding are underlined. The nucleic acid sequences used in this study include:

*GQ (**1**).* 5′-*TTTGGGTAGGGCGGGTTGGG*-3′

*DBA (**6**).* 5′-**GTCTCTGTGTGCGCCAGAGACACTGGGGCAGATATGGGCCAGCACAGAATGAGGCCC**-3′

*Nucleoapzyme (**7**).* 5′-*TTTGGGTAGGGCGGGTTGGG*TATA**GTCTCTGTGTGCGCCAGAGACACTGGGGCAGATATGGGCCAGCACAGAATGAGGCCC**-3′

*Mutated Nucleoapzyme (**7a**).* 5′-*TTTGGGTAGGGCGGGTTGGG*TATA**GTCTCTGTGTGCTTCAGAGACACTGGGGCAGATATGGGCCTGCACAGAATTTGGCCC**-3′

*Scrambled Nucleoapzyme (**7b**).* *TTTGGGTAGGGCGGGTTGGG*TATACGGTAGCTGGCGCGAGTGAGGCAGACGTCCGATGAACCCTGTACTGAGCCGAACTGA

*Nucleoapzyme (**7c**).* 5′-*TTTGGGTAGGGCGGGTTGGG***GTCTCTGTGTGCGCCAGAGACACTGGGGCAGATATGGGCCAGCACAGAATGAGGCCC**-3′

*Nucleoapzyme (**8**).* 5′-**GTCTCTGTGTGCGCCAGAGACACTGGGGCAGATATGGGCCAGCACAGAATGAGGCCC**TATA*TTTGGGTAGGGCGGGTTGGG*-3′

*Nucleoapzyme (**9**).* 5′-**GTCTCTGTGTGCGCCAGAGACACTGGGAA** *TTTGGGTAGGGCGGGTTGGG***AAGCAGATATGGGCCAGCACAGAATGAGGCCC**-3′

*Nucleoapzyme (**10**).* 5′- **GTCTCTGTGTGCGCCAGAGACACTGGGGCAGATATGGGCCAGCACAGAATGAGGCCC**TATA*TTTGGGTAGGGCGGGTTGGG*TATA**GTCTCTGTGTGCGCCAGAGACACTGGGGCAGATATGGGCCAGCACAGAATGAGGCCC**-3′

*1DB6 (**13**).* 5′-***CGACCAACGTGTCGCCTGGTCG***-3′

*1OLD (**14**).* 5′-***ATCGAAACGTAGCGCCTTCGAT***-3′

*2ARG (**15**).* 5′-***TGACCAGGGCAAACGGTAGGTGAGTGGTCA***-3′

*5GQ-2ARG (**16**).* 5′-*TTTGGGTAGGGCGGGTTGGG****TGACCAGGGCAAACGGTAGGTGAGTGGTCA***-3′

*5GQ-1OLD (**17**).* 5′-*TTTGGGTAGGGCGGGTTGGG****ATCGAAACGTAGCGCCTTCGAT***-3′

*5GQ-1DB6 (**18**).* 5′-*TTTGGGTAGGGCGGGTTGGG****CGACCAACGTGTCGCCTGGTCG***-3′

Dopamine Oxidation Studies. *Sample Preparation.* In a typical experiment, MES-buffer solution (5 mM, pH = 5.5, 200 mM $NaNO_3$, 20 mM KNO_3, 5 mM $Mg(NO_3)_2$) was added with a respective DNA strand with a final concentration of 1 μM. The sample was annealed in a block heater at 85 °C for 10 min, and was then allowed to cool-down in a thermostat at 25 °C for 30 min. To this solution, 1 μM of hemin was then added, and the mixture was allowed to equilibrate for additional 30 min at 25 °C to yield the catalytic hemin/G-quadruplex complex. The concentration of the resulting active catalyst, 0.74 μM, was quantified spectroscopically. For a typical oxidation reaction, variable concentrations of dopamine were added, with final concentrations of 0.5, 0.75, 1, 1.5, 2, 3, 5, 20, and 50 μM, followed by the addition of H_2O_2, with a final concentration of 100 μM. Stock solutions of dopamine, L- and D-DOPA were prepared in the MES-buffer solution (5 mM, pH = 5.5, 200 mM $NaNO_3$, 20 mM KNO_3, 5 mM $Mg(NO_3)_2$), and the final concentration of substrate was determined spectroscopically (for dopamine,[43] $\varepsilon(\lambda = 280$ nm$) = 2670$ $M^{-1}\cdot cm^{-1}$; for L- and D-DOPA,[44] $\varepsilon(\lambda = 280$ nm$) = 2630$ $M^{-1}\cdot cm^{-1}$). Dopamine and L- and D-DOPA solutions were stored on ice and were used within 2 h from their preparation.

*Monitoring the Oxidation of Dopamine (**2**), L-DOPA (**11a**), and D-DOPA (**11b**).* The catalytic oxidation of dopamine, L-DOPA, and D-DOPA was followed spectroscopically by measuring the changes in the absorption of the aminochrome product at $\lambda_{max} = 480$ nm for dopamine ($\varepsilon = 3058$ $M^{-1}\cdot cm^{-1}$),[45] or of dopachrome at $\lambda_{max} = 475$ nm ($\varepsilon = 4770$ $M^{-1}\cdot cm^{-1}$)[45] product for L- and D-DOPA. In all measurements, a background signal measured at $\lambda = 800$ nm was subtracted. UV−vis spectroscopy measurements were performed in a quartz cuvette (path length $l = 1$ cm) using a Shimadzu UV-2401PC spectrophotometer.

Kinetic Analysis. The oxidation rate for different systems was determined by fitting a linear trend line to the initial linear region of the different curves. The resulting V_{net} was calculated by subtracting the background oxidation caused by hemin according to $V_{net} = V_{obs} - V_{hemin}$.

DOI: 10.1021/jacs.5b09457
J. Am. Chem. Soc. 2016, 138, 164−172

Dopamine-DBA Affinity. The affinity between the dopamine and the DBA was evaluated by fluorescence anisotropy measurements[29] using a Horiba Jovin Yvon Fluorolog-3 instrument with Fluor Essence.

Oxidation of N-Hydroxy-L-arginine to Citrulline. For a typical experiment, DNA was diluted into HEPES-buffer (100 mM, pH = 8.4, 200 mM KCl, 2 mM $MgCl_2$) to reach a final concentration of 1.25 μM, after which it was annealed at 95 °C for 10 min and was stored in an incubator for 30 min. Then, 1 equiv of hemin (in DMSO) was added and the mixture was incubated again for 30 min. Samples of 50 μL from stock solutions of *N*-hydroxy-L-arginine (5, 2, 1, 0.8, 0.6, 0.4, and 0.1 mM) and 50 μL H_2O_2 (10 mM) were subsequently added to the solution. The progress of the reaction was monitored by taking 60 μL aliquots of the mixture at 0, 1, 2, 4, 8, 16, and 32 min which were quenched by adding to it 150 μL of solution A (3M H_3PO_4, 6M H_2SO_4, 2 mM $NH_4Fe(SO_4)_2$). After all samples were collected, 50 μL of solution B (80 mM 2,3-butanedione monoxime, 2.0 mM thiosemicarbazide) was added. This mixture was heated at 95 °C for 15 min. After cooling the treated mixture to room temperature, the amount of L-citrulline was determined by measuring the absorbance of 170 μL of the stained mixture at λ = 530 nm;[46] the measured absorption was converted into the concentration of L-citrulline using a calibration curve. Formation of L-citrulline was measured in Corning half-area 96-well plates using the BioTek plate-reader (monochromator; path-length correction applied).

Computational Simulations. *Dopamine Oxidizing Nucleoapzymes.* The model of the DBA was constructed using the atomic coordinates of the oligonucleotide generated by MC-Fold/MC-Sym.[47] These coordinates were loaded into the YASARA Structure software package (version 14.8.17);[48] structural constraints as known from literature were implemented in order to generate the kissing loops. A molecular dynamics refinement simulation of the model was run over the time-course of 500 ps using the AMBER03 force field (Figure S11);[49] for this, the simulation cell was automatically filled with water (density: 0.997 g/L, pH = 5.5)[50] and the content of the cell was neutralized using KCl ions. The thus obtained energy-minimized structure of the DBA (Figure S4a) was used in the docking simulations of the various ligands, that is, dopamine (**2**), tyramine, or aminochrome (**3**). For this, the flexible ligand was docked on a rigid aptamer structure 100 times using a built-in macro that applies AutoDock 4.0[51] (grid resolution: 0.375 Å), which uses an empirical scoring system based on the free energy of binding[52] with the Lamarckian Genetic Algorithm.[53] The binding energy is related to the dissociation constant (K_D) by $\Delta G_{bind} = RT \ln(K_D)$. Molecular graphics were created with YASARA (www.yasara.org) and POVRay (www.povray.org).

N-Hydroxy-L-arginine Oxidizing Nucleoapzymes. Three *N*-hydroxy-L-arginine oxidizing nucleoapzyme models were obtained as follows. From the Protein Data Bank (PDB), the NMR-structures of the three aptamer-ligand complexes were received, that is, structures associated with PDB codes 1DB6, 1OLD, and 2ARG. On the 5′-end of the aptamers, the hemin/G-quadruplex structure that was derived from 4FXM.pdb was attached. The in silico generated conjugate was subjected to a 500 ps long molecular dynamics refinement simulation (as was described above for dopamine binding aptamer); the final refined structures are shown in the Supporting Information, Figure S10.

■ ASSOCIATED CONTENT

Supporting Information

The Supporting Information is available free of charge on the ACS Publications website at DOI: 10.1021/jacs.5b09457.

hGQ-mediated time-dependent absorption spectra corresponding to the oxidation of dopamine to aminochrome; cooperativity scheme between the hGQ active site and the DBA binding site; absorbance spectra of the hGQ Soret band of the different nucleoapzymes; additional information about the computational simulations; Enlarged figures of the computational model; potential energy of the different snapshots of the molecular dynamics refinement simulations; cross reactivity activities (PDF)

■ AUTHOR INFORMATION

Corresponding Author

*willnea@vms.huji.ac.il

Author Contributions

†E.G. and H.B.A. contributed equally.

Notes

The authors declare no competing financial interest.

■ ACKNOWLEDGMENTS

This research is supported by the Israel Science Foundation and by The Minerva Center for Biohybrid Complex Systems. We acknowledge the assistance of Prof. G. Haran and R. Kantaev, The Weizmann Institute of Science, Rehovot, in the fluorescence anisotropy measurements.

■ REFERENCES

(1) Silverman, S. K. *Chem. Commun.* **2008**, 3467.
(2) Schlosser, K.; Li, Y. *Chem. Biol.* **2009**, *16*, 311.
(3) Carmi, N.; Balkhi, S. R.; Breaker, R. R. *Proc. Natl. Acad. Sci. U. S. A.* **1998**, *95*, 2233.
(4) Sreedhara, A.; Li, Y.; Breaker, R. R. *J. Am. Chem. Soc.* **2004**, *126*, 3454.
(5) Boersma, A. J.; Megens, R. P.; Feringa, B. L.; Roelfes, G. *Chem. Soc. Rev.* **2010**, *39*, 2083.
(6) Wilking, M.; Hennecke, U. *Org. Biomol. Chem.* **2013**, *11*, 6940.
(7) Megens, R. P.; Roelfes, G. *Chem. Commun.* **2012**, *48*, 6366.
(8) Walsh, S.; Sachdeva, M. A.; Silverman, S. K. *J. Am. Chem. Soc.* **2013**, *135*, 14928.
(9) Travascio, P.; Li, Y.; Sen, D. *Chem. Biol.* **1998**, *5*, 505.
(10) Sen, D.; Poon, L. C. *Crit. Rev. Biochem. Mol. Biol.* **2011**, *46*, 478.
(11) Travascio, P.; Bennet, A. J.; Wang, D. Y.; Sen, D. *Chem. Biol.* **1999**, *6*, 779.
(12) Nakayama, S.; Sintim, H. O. *Mol. BioSyst.* **2011**, *6*, 89.
(13) Pavlov, V.; Xiao, Y.; Gill, R.; Dishon, A.; Kotler, M.; Willner, I. *Anal. Chem.* **2004**, *76*, 2152.
(14) Nakayama, S.; Sintim, H. O. *Anal. Chim. Acta* **2012**, *747*, 1.
(15) Golub, E.; Freeman, R.; Willner, I. *Anal. Chem.* **2013**, *85*, 12126.
(16) Wang, Z. G.; Zhan, P.; Ding, B. *ACS Nano* **2013**, *7*, 1591.
(17) Wang, F.; Lu, C. H.; Willner, I. *Chem. Rev.* **2014**, *114*, 2881.
(18) Willner, I.; Shlyahovsky, B.; Zayats, M.; Willner, B. *Chem. Soc. Rev.* **2008**, *37*, 1153.
(19) Zhao, W. W.; Xu, J. J.; Chen, H. Y. *Chem. Rev.* **2014**, *114*, 7421.
(20) Osborne, S. E.; Ellington, A. D. *Chem. Rev.* **1997**, *97*, 349.
(21) Klussmann, S. *The Aptamer Handbook: Functional Oligonucleotides and Their Applications*; Wiley-VCH: Weinheim, 2006.
(22) Keefe, A. D.; Pai, S.; Ellington, A. D. *Nat. Rev. Drug Discovery* **2010**, *9*, 537.
(23) Cho, E. J.; Lee, J.-W.; Ellington, A. D. *Annu. Rev. Anal. Chem.* **2009**, *2*, 241.
(24) Seelig, B.; Keiper, S.; Stuhlmann, F.; Jäschke, A. *Angew. Chem., Int. Ed.* **2000**, *39*, 4576.
(25) Chun, S.; Jeong, S.; Kim, J.; Chong, B.; Park, Y.; Park, H.; Yu, J. *J. Am. Chem. Soc.* **1999**, *121*, 10844.
(26) Famulok, M.; Hartig, J. S.; Mayer, G. *Chem. Rev.* **2007**, *107*, 3715.
(27) Dokukin, V.; Silverman, S. K. *Chem. Commun.* **2014**, *50*, 9317.
(28) Mannironi, C.; Di Nardo, A.; Fruscoloni, P.; Tocchini-Valentini, G. P. *Biochemistry* **1997**, *36*, 9726.
(29) Walsh, R.; DeRosa, M. C. *Biochem. Biophys. Res. Commun.* **2009**, *388*, 732.
(30) Napolitano, A.; Crescenzi, O.; Pezzella, A.; Prota, G. *J. Med. Chem.* **1995**, *38*, 917.

DOI: 10.1021/jacs.5b09457
J. Am. Chem. Soc. 2016, 138, 164−172

(31) Cornish-Bowden, A. *Fundamentals of Enzyme Kinetics*, 4th ed.; Wiley-Blackwell: Weinheim, 2012.
(32) Purich, D. L.; Allison, R. D. *Handbook of Biochemical Kinetics*; Academic Press: San Diego, CA, 2000.
(33) Li, B. R.; Hsieh, Y. J.; Chen, Y. X.; Chung, Y. T.; Pan, C. Y.; Chen, Y. T. *J. Am. Chem. Soc.* **2013**, *135*, 16034.
(34) Zhang, M.; Li, H.; Deng, M.; Weng, X.; Ma, H.; Feng, S.; Zhou, Y.; Zhou, X. *Chem. Biodiversity* **2012**, *9*, 170.
(35) Mao, X.; Simon, A. J.; Pei, H.; Shi, J.; Li, J.; Huang, Q.; Plaxco, K. W.; Fan, C. *Chem. Sci.* **2016**, DOI: 10.1039/C5SC03705K.
(36) Krieger, E.; Koraimann, G.; Vriend, G. *Proteins: Struct., Funct., Genet.* **2002**, *47*, 393.
(37) Bauke Albada, H.; Rosati, F.; Coquière, D.; Roelfes, G.; Liskamp, R. M. J. *Eur. J. Org. Chem.* **2011**, *2011*, 1714.
(38) Albada, H. B.; Golub, E.; Willner, I. *J. Comput.-Aided Mol. Des.* **2015**, *29*, 643.
(39) Robertson, S. A.; Harada, K.; Frankel, A. D.; Wemmer, D. E. *Biochemistry* **2000**, *39*, 946.
(40) Harada, K.; Frankel, A. D. *Neurourol. Urodyn.* **1995**, *14*, 5798.
(41) Lin, C. H.; Wang, W.; Jones, R. A.; Patel, D. *Chem. Biol.* **1998**, *5*, 555.
(42) Albada, H. B.; Soulimani, F.; Weckhuysen, B. M.; Liskamp, R. M. J. *Chem. Commun.* **2007**, 4895.
(43) Evans, J. P.; Ahn, K.; Klinman, J. P. *J. Biol. Chem.* **2004**, *279*, 5048.
(44) Merck. *The Merck Index*, 13th ed.; O'Neil, M. J., Smith, A., Heckelman, P. E., Budavari, S.; Merck: Kenilworth, NJ, 2001; Entry #5485.
(45) Baez, S.; Segura-Aguilar, J.; Widersten, M.; Johansson, A. S.; Mannervik, B. *Biochem. J.* **1997**, *324*, 25.
(46) Knipp, M.; Vasák, M. *Anal. Biochem.* **2000**, *286*, 257.
(47) Parisien, M.; Major, F. *Nature* **2008**, *452*, 51.
(48) Krieger, E.; Koraimann, G.; Vriend, G. *Proteins: Struct., Funct., Genet.* **2002**, *47*, 393.
(49) Duan, Y.; Wu, C.; Chowdhury, S.; Lee, M. C.; Xiong, G.; Zhang, W.; Yang, R.; Cieplak, P.; Luo, R.; Lee, T.; et al. *J. Comput. Chem.* **2003**, *24*, 1999.
(50) Krieger, E.; Darden, T.; Nabuurs, S.; Finkelstein, A.; Vriend, G. *Proteins: Struct., Funct., Genet.* **2004**, *57*, 678.
(51) Morris, G. M.; Goodsell, D. S.; Halliday, R. S.; Huey, R.; Hart, W. E.; Belew, R. K.; Olson, A. J. *J. Comput. Chem.* **1998**, *19*, 1639.
(52) Huey, R.; Morris, G. M.; Olson, A. J.; Goodsell, D. S. *J. Comput. Chem.* **2007**, *28*, 1145.
(53) Solis, F. J.; Wets, R. J. B. *Math. Oper. Res.* **1981**, *6*, 19.

DOI: 10.1021/jacs.5b09457
J. Am. Chem. Soc. 2016, 138, 164−172